Supporting Information

Tunable direct band gap of β-$CuGaO_2$ and β-$LiGaO_2$ solid solutions in the full visible range

Issei Suzuki, Yuki Mizuno and Takahisa Omata*

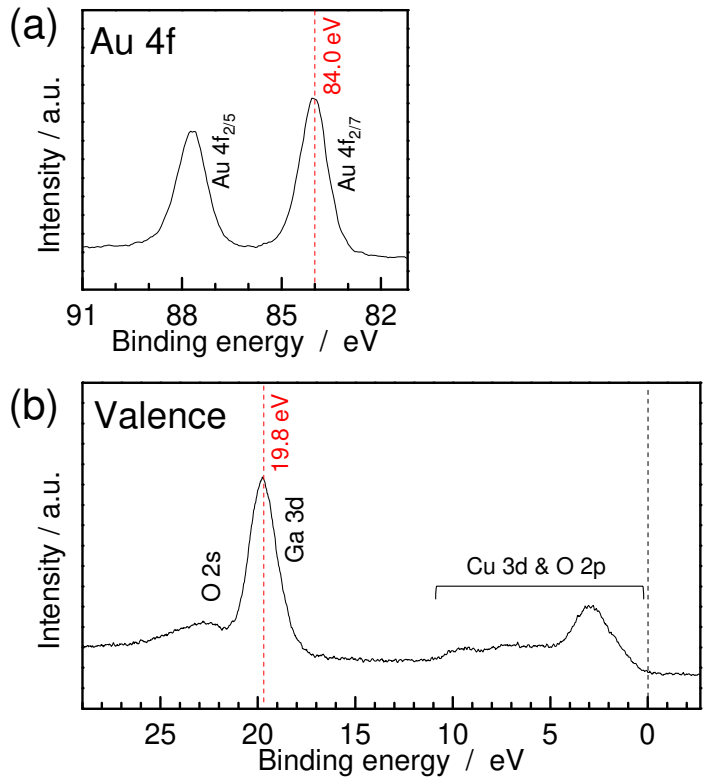

Figure S1. XPS spectra of the β-$CuGaO_2$ compact (80% of the theoretical density), the surface of which was partly sputtered with a Au film. Ag Lα X-ray radiation was used as the excitation source. A detailed description of the preparation of the β-$CuGaO_2$ compact and XPS measurement are available in Ref. [1]. (a) XPS spectrum of the Au 4f core level. The binding energy was calibrated using the Au $4f_{2/7}$ peak at 84.0 eV. (b) XPS spectrum of the valence band of the β-$CuGaO_2$ compact with the calibrated binding energy. The Ga 3d peak was located at 19.8 eV.

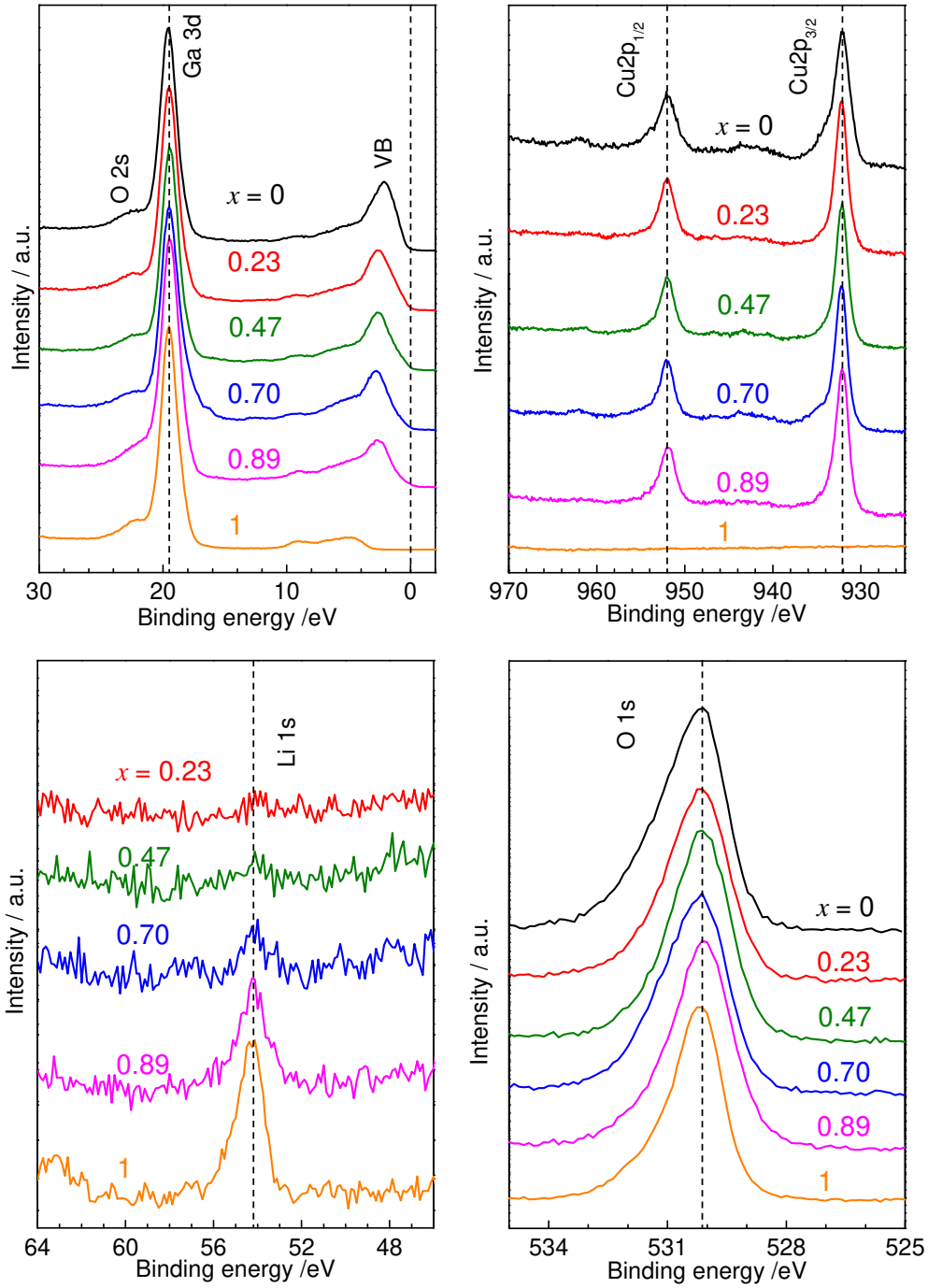

Figure S2. XPS spectra of the valence band, and Ga 3d, Cu 2p, Li 1s and O 1s energy levels of β-($Cu_{1-x}Li_x$)GaO_2. The binding energy was calibrated using the Ga 3d peak at 19.8 eV.

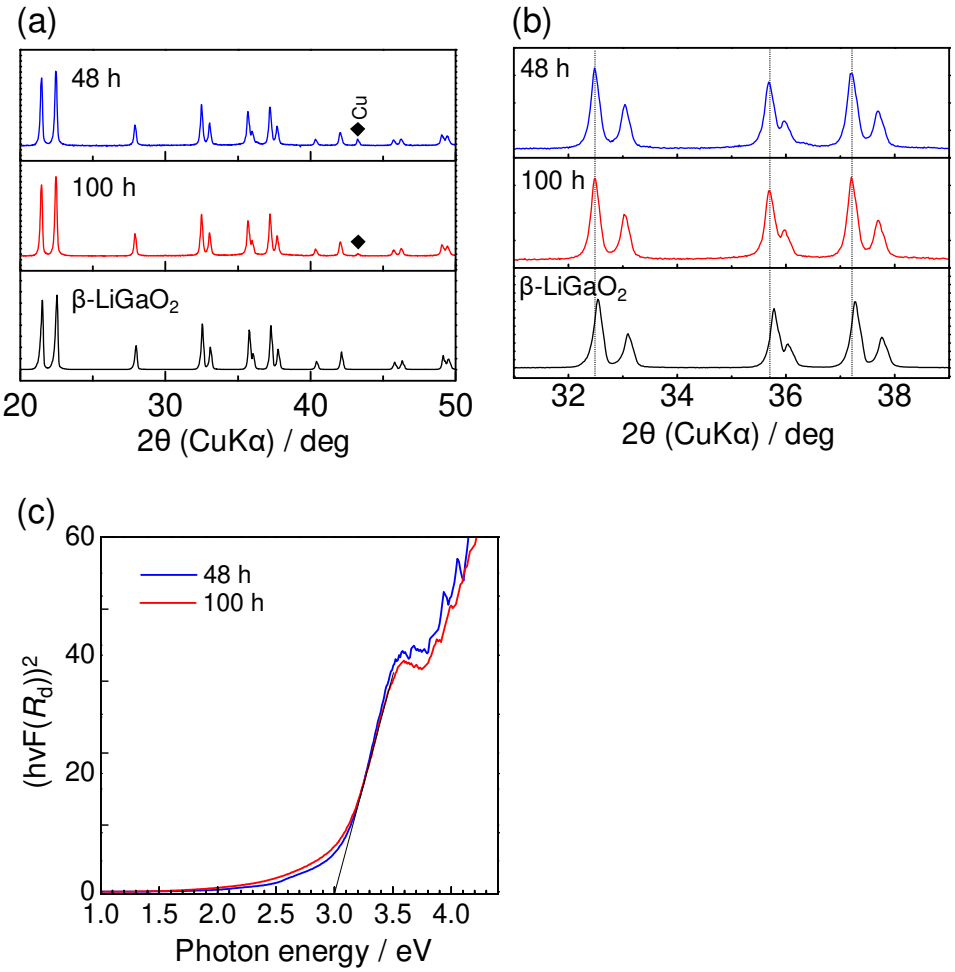

Figure S3 (a) XRD profiles (θ–2θ scan) and (b) its magnified view, and (c) optical absorption spectra of the samples after ion exchange of 48 and 100 hours. The mixing ratio was β-$CuGaO_2$:LiCl = 1:1. The results were completely identical regardless of reaction time, which indicates that prolonging of the reaction times does not promote further ion exchange.

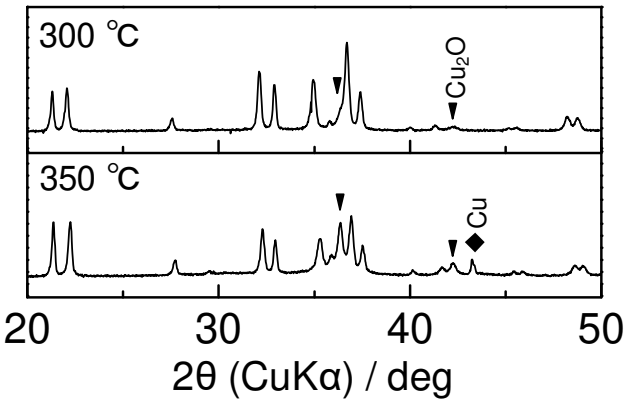

Figure S4. XRD profiles (θ–2θ scan) of the sample after ion exchange (48 h) at 300 and 350 °C. The mixing ratio was β-$CuGaO_2$:LiCl = 1:0.5. The sample collected after ion exchange at 350 °C contained significant amounts of Cu_2O and Cu impurities.

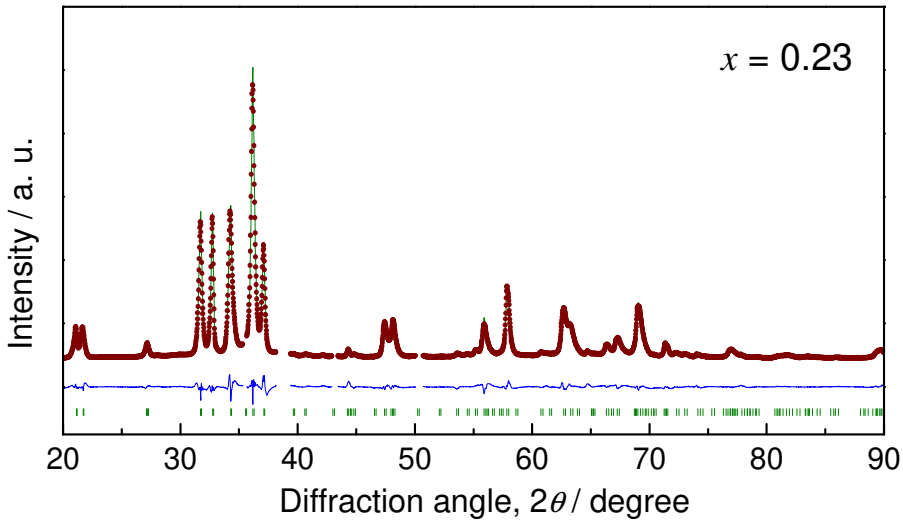

Figure S5. Powder X-ray diffraction and Rietveld plots of β-$(Cu_{0.76}Li_{0.23})O_2$. The solid green line and red dots are the calculated and observed spectra, respectively. The difference between the calculated and observed spectra is plotted with a blue line. The positions of the peaks are marked by green vertical indicators. The profiles of 35.32°–35.66°, 38.16°–39.40°, 38.16°–39.40°, 42.92°–43.44° and 50.06°–50.07° were excluded from the refinement because of diffractions from impurity phases.

Table S1. Structural parameters of β-$(Cu_{0.76}Li_{0.23})O_2$

Space group		$Pna2_1$				
Lattice parameter[Å]		a_0 = 5.46277(9)	b_0 = 6.57579(12)		c_0 = 5.22473(9)	
		Atomic parameter				
Element	Site	*g*	*x*	*y*	*x*	*B*
Cu	4*a*	0.762(2)	0.4391(2)	0.1367(3)	0.4990(3)	1.849(45)
Li	4*a*	0.23	0.4391(2)	0.1367(3)	0.4990(3)	1.849(45)
Ga	4*a*	1	0.0774(2)	0.1296(2)	0	0.534(26)
O(1)	4*a*	1	0.3975(8)	0.1602(7)	0.9013(6)	0.229(74)
O(2)	4*a*	1	0.4282(9)	0.5891(8)	0.8478(6)	0.229(74)
Reliability factors		R_p = 1.667 %, R_{wp} = 2.504 %, R_e = 1.315, S = 1.9040				

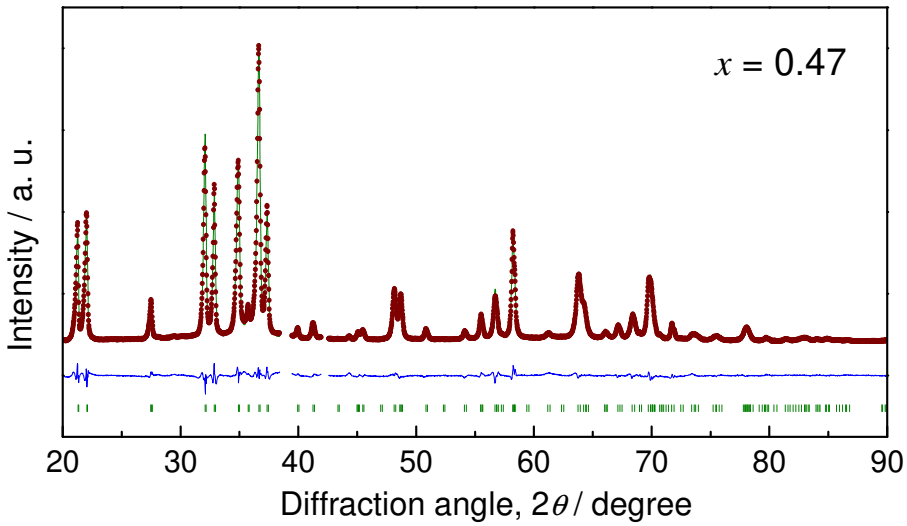

Figure S6. Powder X-ray diffraction and Rietveld plots of β-$(Cu_{0.45}Li_{0.47})O_2$. The profiles of 38.42°–39.46° and 41.94°–42.58° were excluded from the refinement because of diffractions from impurity phases.

Table S2. Structural parameters of β-$(Cu_{0.45}Li_{0.47})O_2$

Space group		$Pna2_1$				
Lattice parameter[Å]		a_0=5.44388(5)		b_0=6.48901(8)		c_0=5.13568(6)
		Atomic parameter				
Element	Site	*g*	*x*	*y*	*x*	*B*
Cu	4*a*	0.452(1)	0.4370(2)	0.1326(3)	0.4982(10)	2.281(39)
Li	4*a*	0.47	0.4370(2)	0.1326(3)	0.4982(10)	2.281(39)
Ga	4*a*	1	0.0793(1)	0.1289(1)	0	0.911(16)
O(1)	4*a*	1	0.4088(5)	0.1540(5)	0.8937(5)	2.022(61)
O(2)	4*a*	1	0.4224(5)	0.6072(6)	0.8576(4)	2.022(61)
Reliability factors		R_p = 1.524 %, R_{wp} = 2.154 %, R_e = 1.367, S = 1.5763				

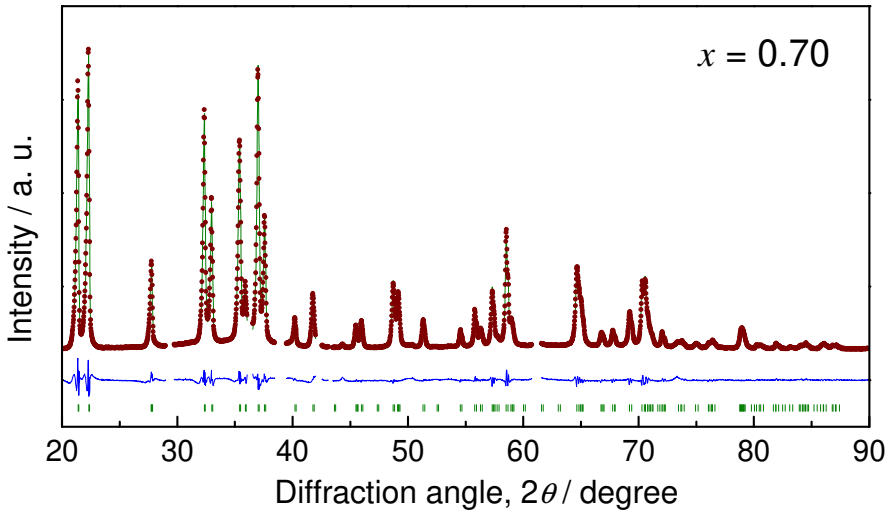

Figure S7. Powder X-ray diffraction and Rietveld plots of β-$(Cu_{0.34}Li_{0.70})O_2$. The profiles of 28.98°–29.72°, 36.06°–36.54°, 38.44°–39.46°, 42.00°–42.54° and 60.74°–61.58° were excluded from the refinement because of diffractions from impurity phases.

Table S3. Structural parameters of β-$(Cu_{0.34}Li_{0.70})O_2$

Space group		$Pna2_1$				
Lattice parameter[Å]		a_0=5.42657(5)		b_0=6.42639(6)		c_0=5.06593(5)
		Atomic parameter				
Element	Site	*g*	*x*	*y*	*x*	*B*
Cu	4*a*	0.180(1)	0.4303(5)	0.1311(5)	0.5048(14)	2.304(62)
Li	4*a*	0.70	0.4303(5)	0.1311(5)	0.5048(14)	2.304(62)
Ga	4*a*	1	0.0820(1)	0.1274(1)	0	1.120(14)
O(1)	4*a*	1	0.4164(5)	0.1434(5)	0.8982(4)	0.925(47)
O(2)	4*a*	1	0.4269(5)	0.6137(6)	0.8705(4)	0.925(47)
Reliability factors		R_p = 1.896 %, R_{wp} = 2.585 %, R_e = 1.488, S = 1.7370				

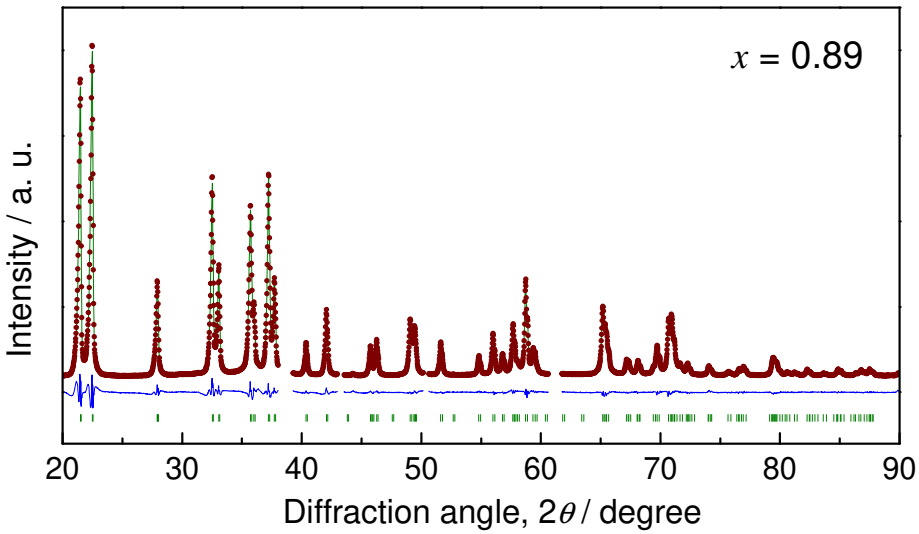

Figure S8. Powder X-ray diffraction and Rietveld plots of β-($Cu_{0.05}Li_{0.89}$)O_2. The profiles of 38.02°–39.26°, 42.98°–43.54°, 50.16°–50.64° and 60.62°–61.76° were excluded from the refinement because of diffractions from impurity phases.

Table S4. Structural parameters of β-($Cu_{0.05}Li_{0.89}$)O_2

Space group		$Pna2_1$				
Lattice parameter[Å]		a_0=5.41259(5)		b_0=6.38917(6)		c_0=5.02358(5)
		Atomic parameter				
Element	Site	*g*	*x*	*y*	*x*	*B*
Cu	4*a*	0.045(2)	0.4214(9)	0.1252(9)	0.4756(23)	2.046(111)
Li	4*a*	0.89	0.4303(5)	0.1311(5)	0.5048(14)	2.046(111)
Ga	4*a*	1	0.0820(1)	0.1260(1)	0	1.071(13)
O(1)	4*a*	1	0.4097(5)	0.1384(5)	0.8957(4)	0.820(44)
O(2)	4*a*	1	0.4308(5)	0.6137(5)	0.8687(4)	0.820(44)
Reliability factors		R_p = 2.356 %, R_{wp} = 3.409 %, R_e = 1.815, S = 1.8785				

[1] Suzuki I, Nagatani H, Kita M, Iguchi Y, Sato C, Yanagi H, Ohashi N and Omata T 2016 First principles calculations of ternary wurtzite β-CuGaO 2 *J. Appl. Phys.* **119** 095701